Effects of Cycle Duration and Test Hardware in Relative Humidity Cycling of a Polymer Electrolyte Membrane

Jixin Chen[1*], Alireza Goshtasbi[1], Amir Peyman Soleymani[2], Mark Ricketts[1], James Waldecker[1], Chunchuan Xu[1], Jun Yang[1], Tulga Ersal[3], Jasna Jankovic[2]

1. Ford Motor Company, Dearborn, Michigan, 48121, USA
2. Center for Clean Energy Engineering, Institute of Materials Science, and Department of Materials Science and Engineering, University of Connecticut, Storrs, Connecticut, 06269, USA
3. Department of Mechanical Engineering, University of Michigan, Ann Arbor, Michigan 48109, USA

* Corresponding Author: jchen186@ford.com

Abstract

In this study, relative humidity (RH) cycling accelerated stress testing (AST) is pursued on a supplier's catalyst coated membrane (CCM). The experimental design includes three RH cycles and two test cell / membrane electrode assembly (MEA) formats. All three cycles tested are shorter than the Department of Energy (DOE) protocol and model simulations indicate that deep and fast hydration swings could still be retained. Edge failure is observed in one test cell, which is in part responsible for the shorter lifetime in RH cycling as compared to using another test cell and suggests a test hardware harmonization if the lifetime is referenced to a target or compared between different materials. Nevertheless, the trends of H_2 crossover versus the number of cycles and overall test time remain consistent for two hardware formats. This finding suggests that RH cycling could be effectively used to investigate a control factor, such as cycle duration, based on a single hardware and material, towards the development of system strategies on a fuel cell vehicle. Furthermore, since the H_2 crossover versus RH cycling test time plots exhibit clear separation for three cycles, the frequency and duration of cycles both play a role in determining the membrane lifetime.

Key Words: fuel cell, polymer electrolyte membrane, relative humidity cycling, mechanical durability, accelerated stress testing

1. Introduction

Mechanical failure of a polymer electrolyte membrane in the form of cracks, pin-holes and delamination has been identified as a limiting factor in the durability of the fuel cell. The hydration/dehydration cycling of the membrane during the fuel cell operation and the resulting mechanical stress are in part responsible for the mechanical failures [1-5]. Because it could take thousands of hours with various hydration conditions and coupling effects to fail a fuel cell membrane in a vehicle, accelerated stress testing (AST) has been developed to focus on the mechanical stability of a fuel cell membrane. As a typical membrane AST, relative humidity (RH) cycling has been used for lifetime screening [6]. The protocol from the Department of Energy (DOE) or US DRIVE Fuel Cell Tech Team [7] suggests cycling the RH between an over-saturated condition and a dry condition using air or nitrogen. Each cycle consists of flowing air/nitrogen through a humidifier at 90°C dew point for 2 minutes, and then bypassing the humidifier for 2 minutes. The fuel cell is to be maintained at 80°C without back pressure. One could calculate to obtain that the actual RH during the dry phase is only ~3%, and an over-saturation is achieved during the wet phase. The condition of the membrane is to be monitored by periodic diagnostics including H_2 crossover and shorting resistance. A membrane failure is usually captured by an abruptly increased H_2 crossover current (>15 mA/cm^2) as referenced to previous H_2 crossover measurements.

RH cycling between over-saturated and fully dry conditions represents an extreme of a hydration cycle that is rarely experienced in actual operation of a fuel cell vehicle. The induced high mechanical stress on the membrane is thus expected to fail a membrane much sooner than actual field operation. Due to this accelerated nature, RH cycling is widely used in fuel cell membrane development as one of the material screening tests focusing on the mechanical stability. The passing criterion of the DOE protocol is 20,000 cycles, which in theory translates the DOE durability target in field operation to the requirement under a single stressor. For many modern membranes, RH cycling based on the DOE protocol went

through 20,000 cycles without a failure [6, 8]. In other words, RH cycling in air/air or N_2/N_2 is arguably too mild to distinguish membranes, which has reduced the effectiveness of the test as a durability screening tool. To further accelerate the degradation rate, many previous efforts instead focused on RH cycling in H_2/air condition either under a quasi-OCV condition [9, 10] or with a current load [11-13], which becomes a combined mechanical and chemical stress AST. In a recent study of the combined AST [14], RH cycling was achieved through cycling current on an integral cell with the capability of local current and HFR measurements. However, the relative roles of mechanical stressor and chemical stressor in a combined AST are not fully understood yet given the complexity of their synergistic effects [15]. Therefore, the mechanical behaviors of a membrane cannot be effectively examined with the combined AST, although it is an efficient screening tool.

Besides the wide use of RH cycling as a screening test, a few prior works in the literature have focused on some of the control factors in this test. For example, Mukundan et al. [8] have used a shorter RH cycle of 45 s dry and 30 s wet in H_2/air, which increased the number of hygral variations per unit time by a factor of 3 despite a ~25% reduction in the magnitude of hygral change during each cycle. Lai et al. [2] conducted in-situ humidity cycling tests on different membranes exposed to various RH swings from 0%, 50%, and 80%, respectively, to 150%, and found longer time-to-failure to be associated with smaller humidity swing. Alavijeh et al. [16] examined 2 min wet (90% RH) and 2 min dry (0% RH) cycle at 80°C versus 1 min wet (100% RH) and 3 min dry (0% RH) cycle at 95°C. It was found that the latter led to more severe mechanical damage due to the higher temperature and larger fatigue stress amplitude.

While these studies have covered different aspects of RH cycling, a systematic study on RH cycle duration and frequency cannot be found in the literature. However, such a study could shed light on the mechanical lifetime determining factors and contribute to the development of system strategies on a

fuel cell vehicle. For instance, on a blister or ex-situ membrane mechanical test [17], it was reported that fatigue cycling (10 s with pressure and 4 s without pressure) and creep to leak (holding constant pressure until leak) led to almost identical lifetimes, which was observed for three membranes. Thus, it was the time under load rather than the cycling effect that appeared important. An in-situ RH cycling study focusing on cycle duration at a fixed percentage of wet/dry time would verify if this finding holds true for reinforced membranes under hydration cycling in a fuel cell. More importantly, system strategies must be considered along with material solutions for durability enhancement from an automotive OEM's perspective. The membrane mechanical lifetime data under various RH cycles could provide an important design guide for system hydration controls.

Furthermore, although the DOE RH cycling protocol is widely accepted, standard test cell hardware has not been universally adopted. In one study, a 50 cm^2 single cell fixture from Fuel Cell Technologies, Inc. has been used [8], which features a multi-serpentine flow field [18] and gasket sealing. Another study used a short stack of 5 cells with co-flow parallel straight channels and 45 cm^2 active area [16]. It appears that the impact of cell hardware on RH cycling outcome has been overlooked, as a comparative study under the same protocol does not exist in the literature to the best of the authors' knowledge. It is of the authors' interest to explore this impact, as well as the different failure modes, if any, associated with the cell hardware and sealing method.

In this work, a systematic RH cycling test was performed on a supplier's catalyst coated membrane (CCM), with an expectation of gaining insights on the mechanical behaviors of a state-of-art membrane that can be used for the development of system strategies towards enhanced durability. Unlike a component supplier who may simply adopt the RH cycling as a screening tool, it was of the authors' interest to adopt this test towards a design tool for system strategies. With these motivations, three RH

cycles and two test cell hardware were used to create a 2x3 experimental design. The cycle duration was varied from the DOE protocol while maintaining the other operating conditions to ensure that the results are not affected by the chemical stressor and the synergistic effects that are otherwise present in a combined AST. The membrane failures were observed from all 6 cases in about 2-3 weeks, enabling repetitions of this experimental study as needed, which are important as membrane fatigue data could vary significantly [17, 19]. The failed membrane samples from RH cycling were removed for inspection of failure modes. In the following, the test hardware and procedures are introduced, with a discussion of the experimental results. A summary of the findings and contributions is provided at the end.

2. Experimental

2.1 Material and Test Hardware

In this study, CCMs from a supplier were tested, which contained a ~16.6 µm reinforced perfluorinated sulfonic acid (PFSA) membrane and state-of-art catalysts. Two test cell / MEA formats were used. The first one was a commercially available 50 cm^2 Fuel Cell Technologies (FCT) cell [18]. Figure 1(a) shows an image of the FCT cell and the corresponding MEA. The MEA has the same size as the active area with a surrounding Teflon® hard-fit gasket. The GDL covers the active area only. The CCM was sandwiched by the GDL in the active area and by the Teflon gasket at the perimeter. The FCT cell was assembled with a torque wrench to maintain consistent compression. Another test cell, the Core Attribute Tester (CAT) cell, was from an internal design and can be seen in Fig. 1(b). The CAT cell has an active area of 48.4 cm^2 and straight flow channels. The engineered gasketing in the CAT cell covers both CCM and GDL at the edges of the active area. In other words, the GDL is slightly larger than the active area, extending underneath the MEA frame. Both cells are considered differential cells and thus suitable for sub-scale AST, although the MEA edge designs are different.

(a)

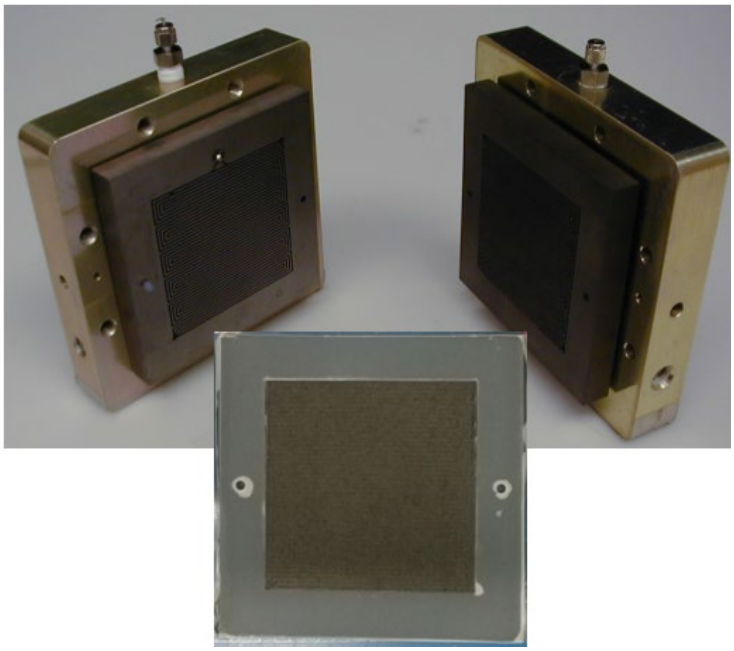

(b)

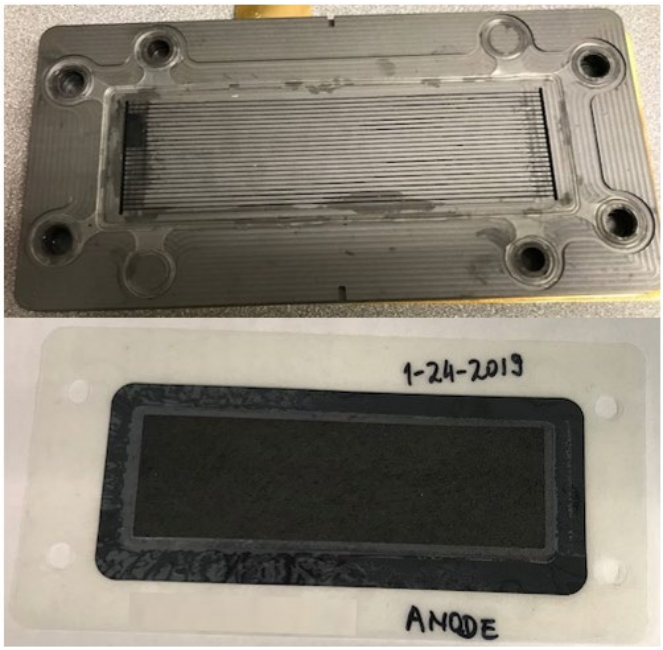

Fig. 1. (a) 50 cm^2 Fuel Cell Technologies (FCT) cell and MEA with gasket; (b) 48.4 cm^2 Core Attribute Tester (CAT) cell and framed MEA.

2.2 RH Cycling Experimental Design

During RH cycling, no back pressure was applied at anode or cathode. The cell was maintained at 80°C, and the humidifier was at 90°C for anode and cathode to achieve an over-saturation or "wet" phase. Air was flowing through anode and cathode with a flow rate of 2 L/min, and periodically bypassing the humidifier to achieve a "dry" phase. Three different RH cycles were tested. The baseline cycle consisted of 45 s dry phase and 30 s wet phase following a recent work from Los Alamos National Laboratory [8], which was found to increase the number of hygral variations per unit time by a factor of 3 compared to the DOE protocol. It was thus expected that the baseline cycle could be more efficient to fail a membrane mechanically. The X2 cycle consisted of 90 s dry phase and 60 s wet phase, and the X0.67 cycle comprised 30 s dry phase and 20 s wet phase. Thus, the time percentage under dry and wet phases is identical for the three cycles, but the cycling frequency or cycle duration is different. The dry phase was longer than the wet phase to allow sufficient time for drying the over-saturated flow field and MEA through humidifier bypass. A longer dry phase would also expose the membrane to longer and greater in-plane tensile stress, thereby reducing its lifetime and the experimental resources needed to induce failure. A simulation using a mathematical model described in [20] has been carried out to confirm that all three cycles are able to achieve a deep and fast hydration swing as shown in Fig. 2, where the ionomer water contents (λ) at anode catalyst layer, cathode catalyst layer and membrane are plotted in response to the RH change in the channel for the baseline cycle. The hydration in the ionomer changes following the RH transient in the channel with a lag no more than two seconds, therefore retaining the deep and fast swing. This feature is available for all three cycles, since only minor differences in λ response exist among the three cycles, as shown in Fig. 2(b). These RH cycles were implemented on two test cell hardware to explore the impacts of cycle duration as well as test cell hardware on the lifetime. Thus, a 2x3 experimental design was pursued for RH cycling as summarized in Table 1. Two fuel cell test

stands with humidifier bypass were used, Station A for FCT cell and Station B for CAT cell. They are identical test stands for simultaneous testing with minor variations.

	Dry	Wet	Note
Station A / FCT	30 s	20 s	X0.67 Cycle
	45 s	30 s	Baseline Cycle
	90 s	60 s	X2 Cycle
Station B / CAT	30 s	20 s	X0.67 Cycle
	45 s	30 s	Baseline Cycle
	90 s	60 s	X2 Cycle

Table 1. The Design of Experiment (DOE) of two test cells and three RH cycles

(a)

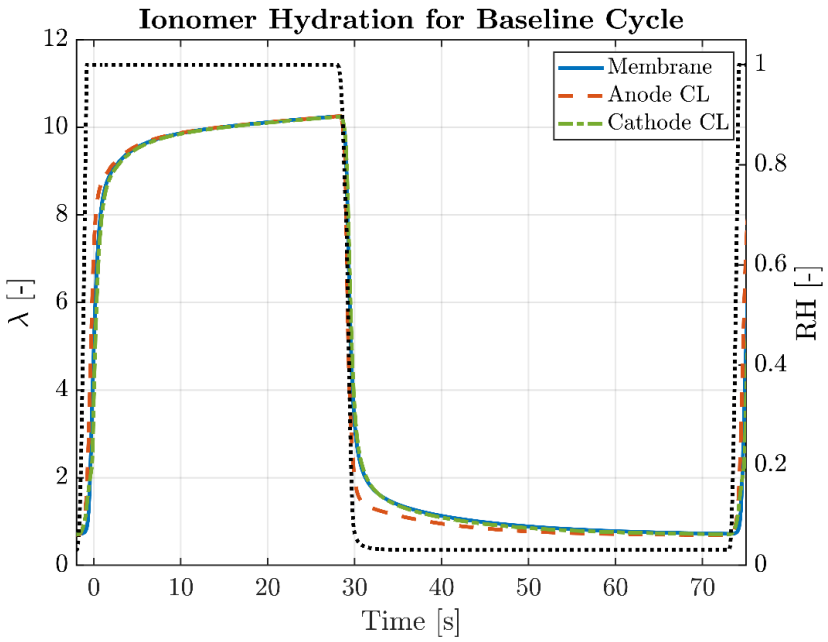

(b)

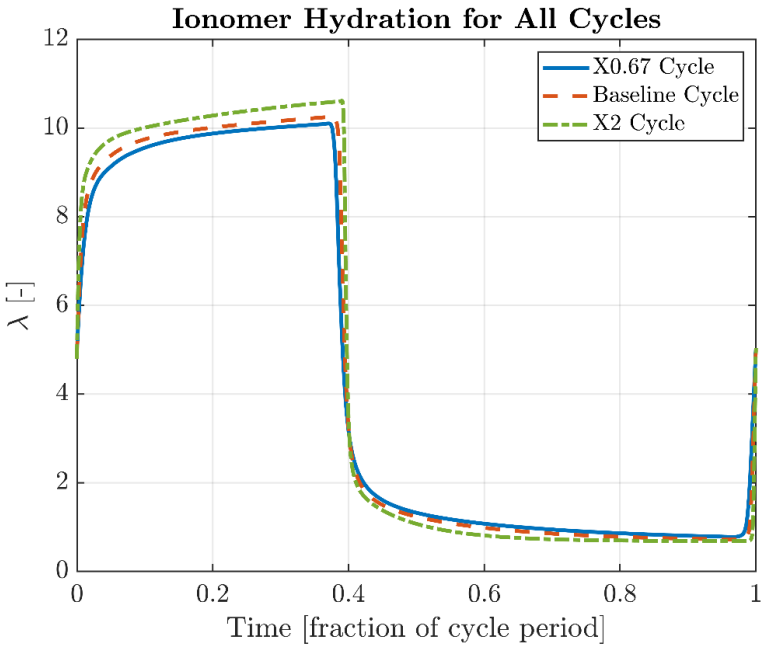

Fig. 2. Simulation of ionomer water content (λ) profiles under three RH cycles. (a) λ evolutions in the membrane, anode catalyst layer, and cathode catalyst layer in response to the RH change in the channel for the baseline cycle. (b) The coplot of membrane λ evolutions for the three cycles. The details of the simulation model can be found in Ref. [20].

2.3 Diagnostics

The RH cycling was periodically interrupted for diagnostics of the membrane condition [7]. H_2 crossover was measured with fully-humidified H_2 in the anode (reference electrode) and fully-humidified N_2 in the cathode (working electrode). The anode back pressure was 160 kPa and the cathode was at 150 kPa, both with 2 L/min flow. The fuel cell was maintained at 80°C. After reaching a steady-state, a cyclic voltammetry scan was performed from 0.05 V to 0.6 V between working and reference electrodes with a scan rate of 20 mV/s. The averaged current density at 0.4 V during cyclic voltammetry scan was taken to quantify the amount of H_2 crossover. In general, the diagnostics were performed every 2-3 days. When approaching end-of-life with an observation of increased H_2 crossover, more frequent diagnostics such as daily diagnostics were performed to capture the failure time more accurately, except for weekends. The failure of the membrane was defined by an H_2 crossover current high enough that would prevent the instrument from completing the cyclic voltammetry scan in measuring H_2 crossover due to reaching the current limit (1 A) of the instrument (BioLogic VSP Potentiostat/Galvanostats). Thus, the H_2 crossover current density at the failure or final diagnostic may be a projected number, as the cyclic voltammetry scan may have stopped prior to reaching 0.4 V. If a substantial increase of H_2 crossover was observed as referenced to beginning-of-life (BOL) and the membrane was suspected to have approached or reached its lifetime, the open circuit voltage (OCV) was measured with increasing anode (H_2) pressure while maintaining constant cathode (air) pressure, to provide secondary information regarding the membrane condition.

The representative data for OCV sensitivity with differential pressure are shown in Fig. 3. At BOL, the OCV showed minor changes as anode pressure increased, as can be seen from Fig. 3(a), where cell voltage exhibited only a few mV drop when the anode pressure increased from 150 to 180 kPa and cathode pressure maintained at 150 kPa. As end-of-life (EOL) was approached, the OCV dropped substantially with increasing anode pressure due to the mechanical defects such as cracks developed

during RH cycling [16, 21, 22] and the consequently increased H_2 crossover, as can be seen from Fig. 3(b). At EOL, such effects became more pronounced as shown in Fig. 3(c).

(a)

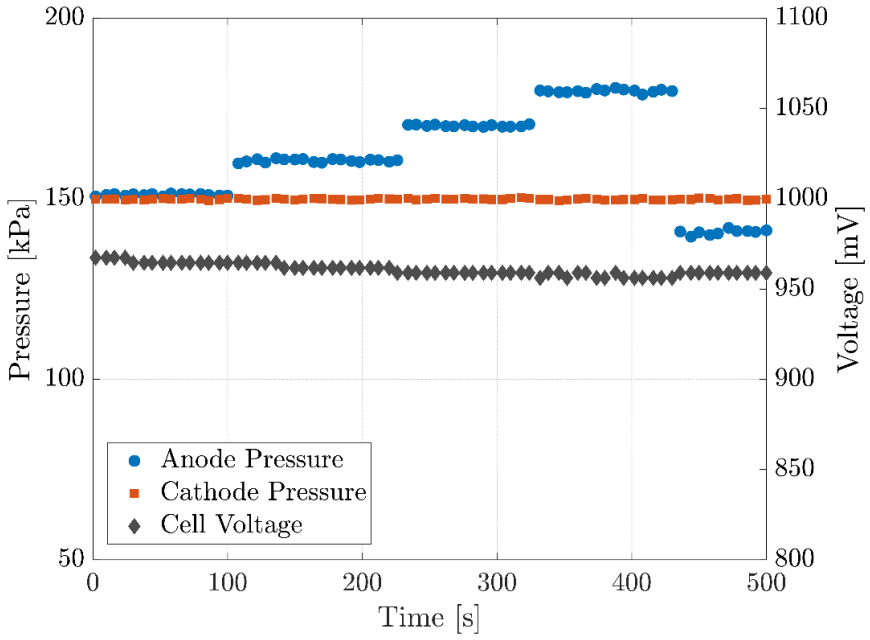

(b)

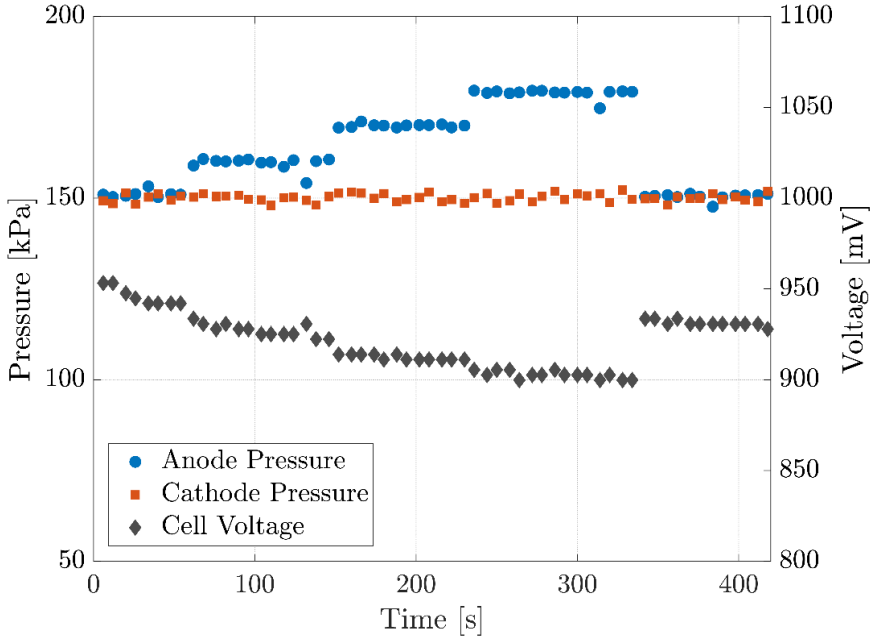

(c)

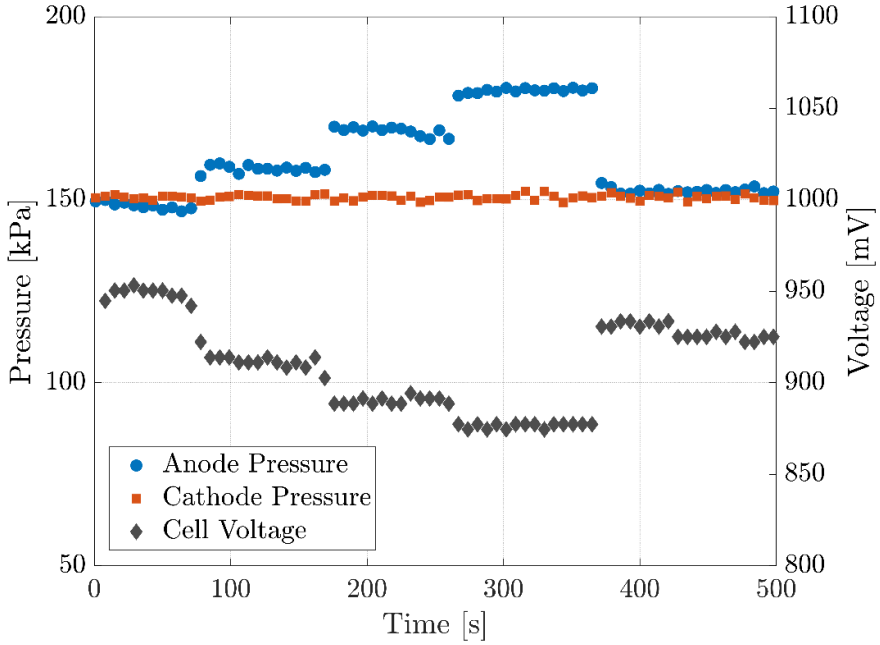

Fig. 3. OCV sensitivity with increasing anode pressure while maintaining a constant cathode pressure, (a) BOL; (b) the diagnostic before EOL; (c) EOL. The cell was at 80°C with 100% RH and 2 L/min reactants at both sides.

2.4 Failure Analysis

Failure analysis was performed on failed MEA samples from the CAT cell. The MEA sample was first sealed in a bubble jig for leakage check. An air pressure of 2 psi was applied to the inlet of the jig. If a pinhole or a defect allowing gas crossover is located, air bubbles would emanate from that spot. A large leakage is defined with bubbles forming in less than 1 second, a small leakage with bubbles forming in more than 10 seconds, and the others are medium leakages. Failure analysis was not performed on failed samples from the FCT cell, as a visual inspection had identified obvious deformations at the edge of the MEA active area where the GDL interfaces with the sealing gasket.

To understand the details of the failure, X-ray Computed Tomography (XCT) and Scanning Electron Microscopy (SEM) were further performed on the identified failure spots from the bubble jig. XCT is being increasingly used for fuel cell electrode and membrane characterization, with a distinct advantage

that non-destructive imaging of the internal structures can be carried out [21-24]. A rectangular 20 mm × 10 mm piece was cut from the MEA, containing the identified bubble spot. The piece was mounted on the holder of a commercial micro-XCT (ZEISS Xradia 520 Versa, Germany) so that the identified failure spot was in the center of the scan. In order to achieve the best contrast in the scans with no filter on the X-ray beam and 4 s exposure time, the electron accelerating voltage and power were 90kV and 8W, respectively. The source and detector distance were adjusted to ensure the pixel size of 2.5 µm for a 2.5×2.5×d mm^3 scan volume (where d is the thickness of the MEA). To scan a larger area, two scans were collected, reconstructed and stitched to create the final 5×2.5×d mm^3 scan volume with 1601 projections per scan. After the XCT analysis, the same section was embedded in EpoThin epoxy resin, polished with the Struers LaboPro-5 polishing system and gold coated using Denton vacuum coater. The Thermo Fisher Scientific Teneo LV Scanning Electron Microscope (SEM) was used to acquire cross-sectional SEM images by the circumferential backscattered (CBS) detector at electron accelerating voltage and beam current of 15 kV and 0.8 nA, respectively.

3. Results and Discussion

3.1 H_2 Crossover versus Cycle Number

The RH cycling results from the FCT cell / Station A are plotted as H_2 crossover versus cycle number in Fig. 4(a), where each cycling protocol was repeated using a fresh CCM for a total of 6 runs. While RH cycling ASTs are not commonly repeated in the literature probably due to the high resources needed, the tests on the FCT cell have been repeated. This is motivated by the fact that typical membrane mechanical fatigue data could scatter significantly [17, 19] as well as the edge failure observed (discussion follows). As seen in the figure, good repeatability has been achieved. The data exhibit three groups corresponding to three cycles. The longest cycle (X2 Cycle) leads to the fewest number of cycles

to fail the membrane, and the shortest cycle (X0.67 Cycle) leads to the greatest number of cycles. While it appears that the X0.67 cycle led to failures of the highest H_2 crossover, these crossover currents are projected values, as the cyclic voltammetry scan did not complete due to the limit of the instrument. It should be noted that the H_2 crossover plots in Fig. 4 are to indicate the time of the failure. As long as an abrupt increase to a high crossover was observed, it was considered a failure. The exact value of the H_2 crossover current was not nearly as important as the occurrence of the abrupt increase in H_2 crossover as an indicator of membrane failure, because such an abrupt increase over the previous low crossovers was typically obvious to show the failure time. Furthermore, although a distributed crossover measurement technique exists in the literature [14], it was not adopted in this work; since the intention was to use RH cycling as a design tool for system strategy development. The H_2 crossover in this work was a lumped measurement for the whole active area, which was a common diagnostic technique and unable to detect the location of failure.

Therefore, the FCT cells had been disassembled to examine the failed MEA samples. As shown in Fig. 5, deformation and/or discontinuity at a few locations around the edge of the GDL and gasket was clearly visible and detectable for all failed samples, which is believed to be the cause of high H_2 crossover and membrane failure. There are a few possible reasons for the edge failure. The gasket, GDL and CCM interfaced at the edge have different responses to hydration cycling due to different material properties, thereby creating a stress concentration [25]. Similar to a mechanical failure in the active area, the cyclic fatigue due to the hydration cycling is also applicable at the edge. Early modeling work has found that the plastic deformation and peak stress during transition are higher at the edge than in the active area [26, 27]. Another vulnerability pertains to the compression from GDL pushing the membrane towards the edge, which is subject to bending against the rigid gasket [28]. A combination of these factors could have led to the observed edge failure, which is part of the motivation of repeating FCT cell runs. As mentioned, repeatability has been found for both failure mode and lifetime.

Figure 4(b) summarizes the RH cycling results from the CAT cell / Station B as H_2 crossover versus cycle number. Similar to the FCT cell results in Fig. 4(a), the X2 Cycle run exhibits fewest number of cycles to fail the membrane, whereas the X0.67 Cycle run exhibits greatest number of cycles. A bubble jig test was performed to identify the failure spot(s) on the CAT cell failed samples, which could not be found by visual inspection. This post-mortem analysis has found the failure spots with medium leakage in the active area of a CAT cell MEA from the baseline cycle and small leakage from the X0.67 Cycle, as well as medium and small leakages from the X2 Cycle, as illustrated in Fig. 6. The multiple leakage spots on the X2 Cycle failed sample could be attributed to the longer lifetime of that sample, which allowed more opportunities to develop a crack. Figure 7 shows the representative SEM and XCT images at BOL and images collected around the failure spot after the RH cycling test. BOL images (Fig. 7(a) and Fig. 7(c)) show an intact CCM without any visible crack, despite some surface wrinkles probably from the manufacturing process. On the post-mortem SEM images (Fig. 7(b)), cracks on the catalyst layer and partially through the membrane can be seen. XCT scans (Fig. 7(d)) further revealed circular defects protruding through the whole CCM thickness, which could be associated with the merging of multiple cracks. These defects exhibit similar morphology as compared to what has been reported previously [22] and they are probably responsible for the observed high crossover and leakage.

(a)

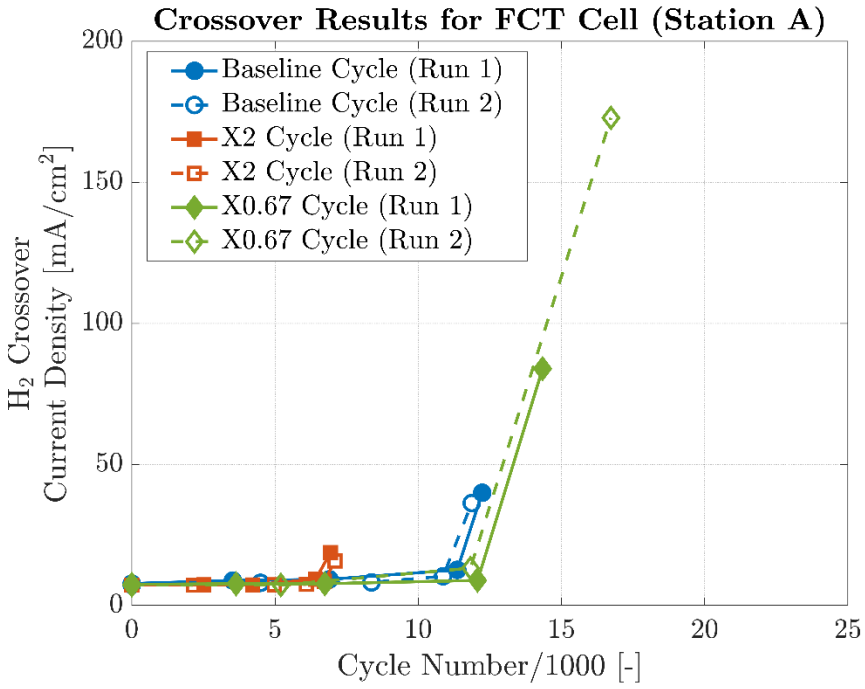

(b)

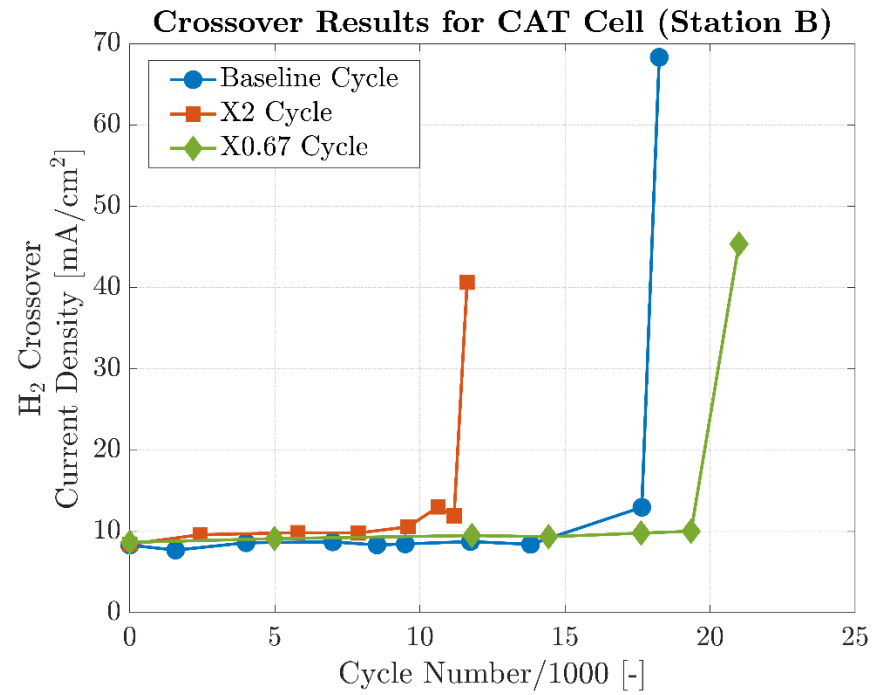

Fig. 4. Evolution of H_2 crossover with cycle number for three RH cycles on (a) Station A / FCT cell; (b) Station B / CAT cell.

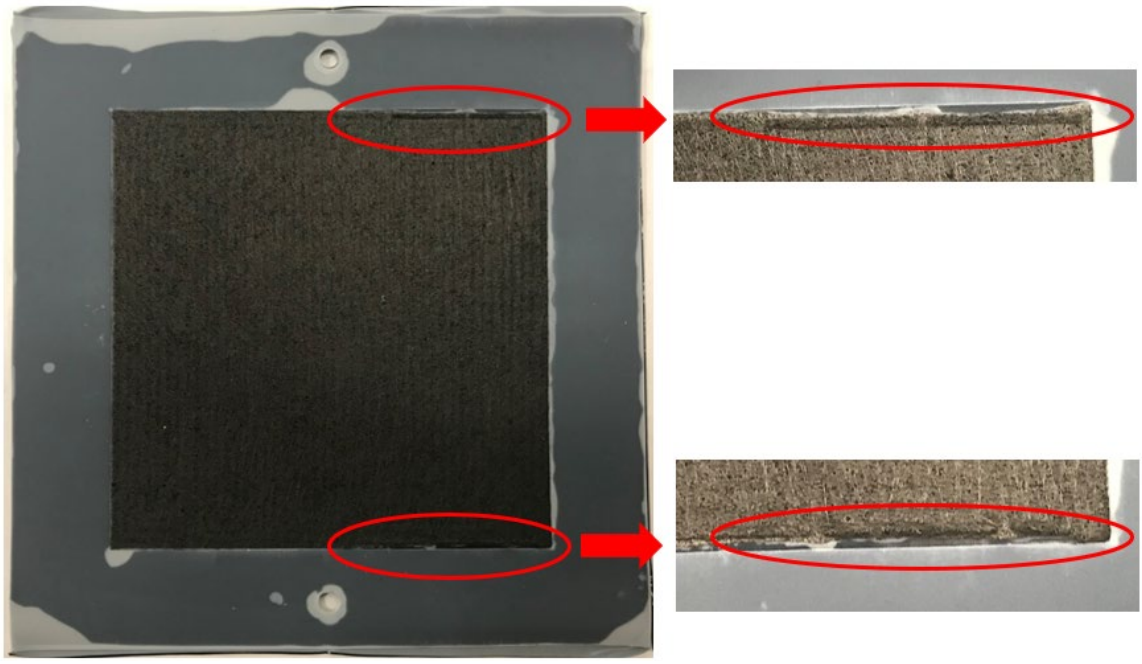

Fig. 5. Edge failures from an FCT cell MEA

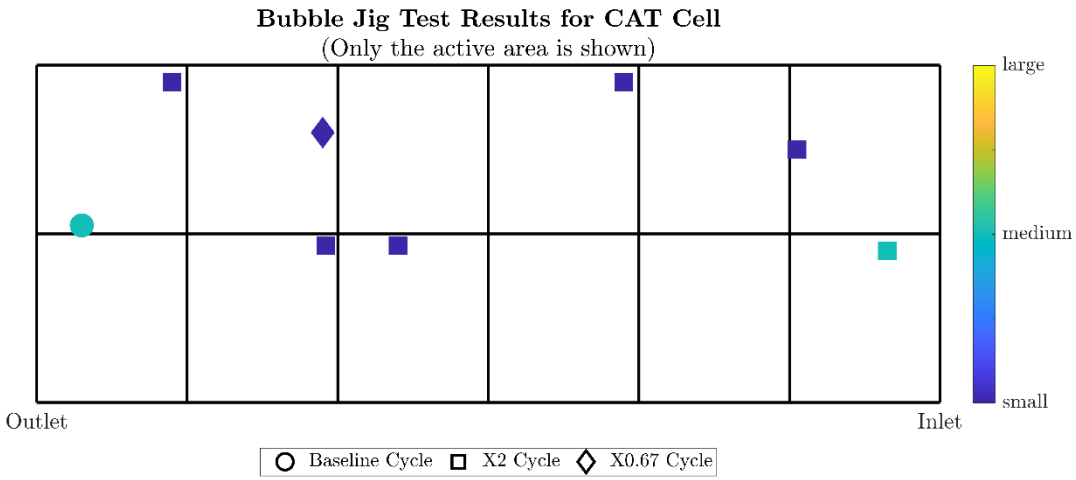

Fig. 6. Bubble jig schematic showing failure spots on the CAT cell membrane from the three cycles. The scale bar illustrates the level of leakage and mechanical failure.

The failure mode is a clear distinction from the CAT cell to the FCT cell where an edge failure was observed, due to the engineered frame for CAT cell sealing. The CAT cell's cycle number until failure is

therefore greater than the corresponding case for FCT cell when Fig. 4(b) and Fig. 4(a) are compared. Nevertheless, a consistent trend of three cycles can be seen regardless of cell format, namely, the longest cycle (X2 Cycle) leads to the fewest number of cycles to fail the membrane and the shortest cycle (X0.67 Cycle) leads to the greatest number of cycles to fail the membrane. Therefore, it seems that the cyclic fatigue due to hydration cycling applicable to both the edge and active area, is the major contributor to the edge failure over the other factors. Under the same mechanism, the higher peak stress at the edge than in the active area could explain the shorter lifetime on an FCT cell as well as the consistent trend for three cycles on two hardware formats. If the RH cycling test is utilized as a design tool focusing on a control factor such as cycle duration and a single material, then a hardware leading to an edge failure would probably be able to capture the impact of that control factor similar to another hardware that results in a failure in the active area. The hardware harmonization is therefore secondary. On the other hand, if it is used to determine the actual lifetime of a specific material, either for durability screening against the target or for comparing different materials, then the hardware format and the gasket design are important factors influencing the lifetime, which should be harmonized or at least considered when cross-referencing tests. For instance, a failure due to unprotected edge should not be compared with a failure in active area from a framed MEA. In summary, harmonization of the test hardware in addition to the test protocol is needed for RH cycling if the actual lifetime is used for comparison or screening, while some literature reports merely the cycle number as lifetime without the details of the test cell and MEA.

(a)

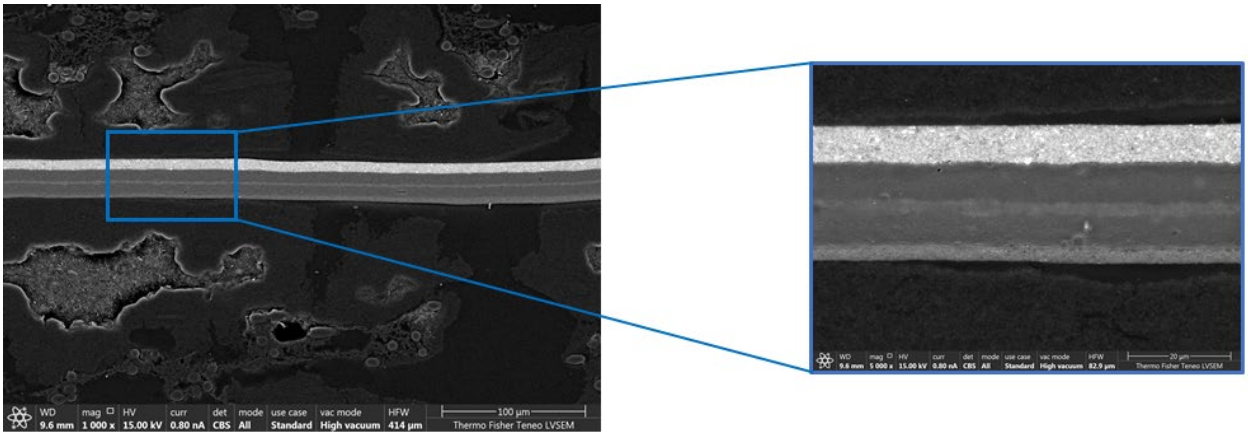
WD mag HV curr det mode use case vac mode HFW
9.6 mm 1 000 x 15.00 kV 0.80 nA CBS All Standard High vacuum 414 µm
100 µm
Thermo Fisher Teneo LVSEM

(b)

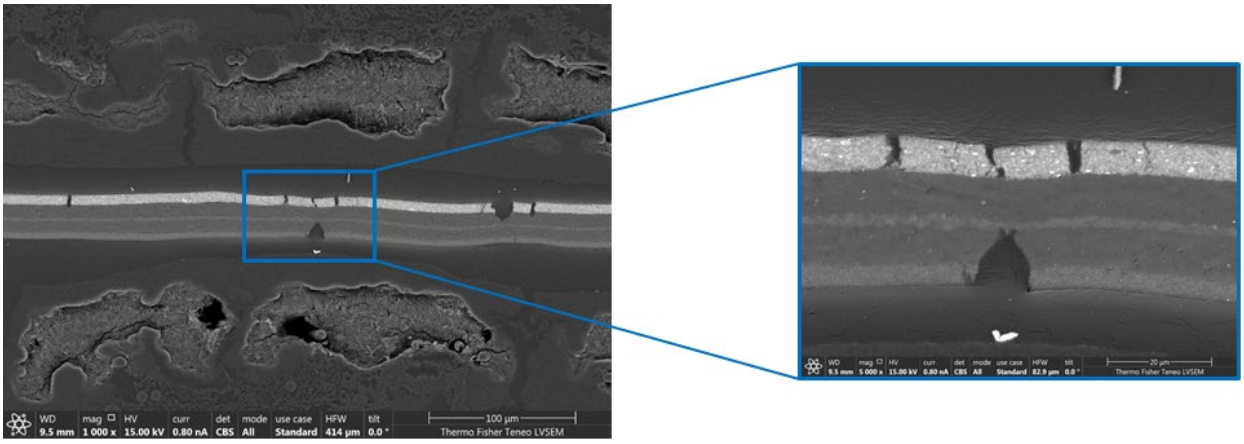
WD mag HV curr det mode use case HFW tilt
9.5 mm 1 000 x 15.00 kV 0.80 nA CBS All Standard 414 µm 0.0 °
100 µm
Thermo Fisher Teneo LVSEM

(c)

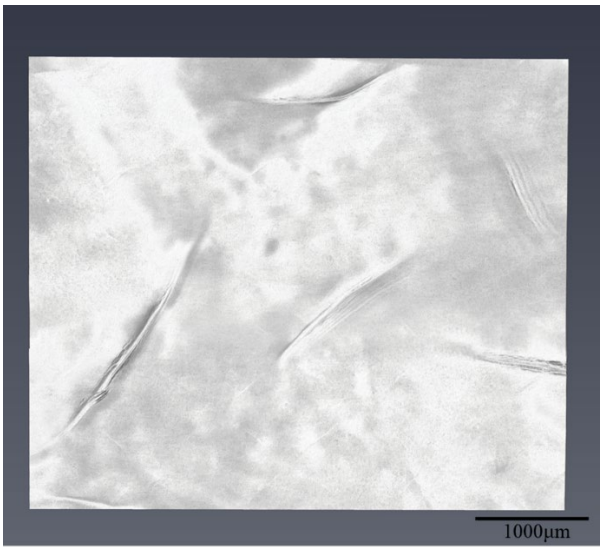
1000µm

(d)

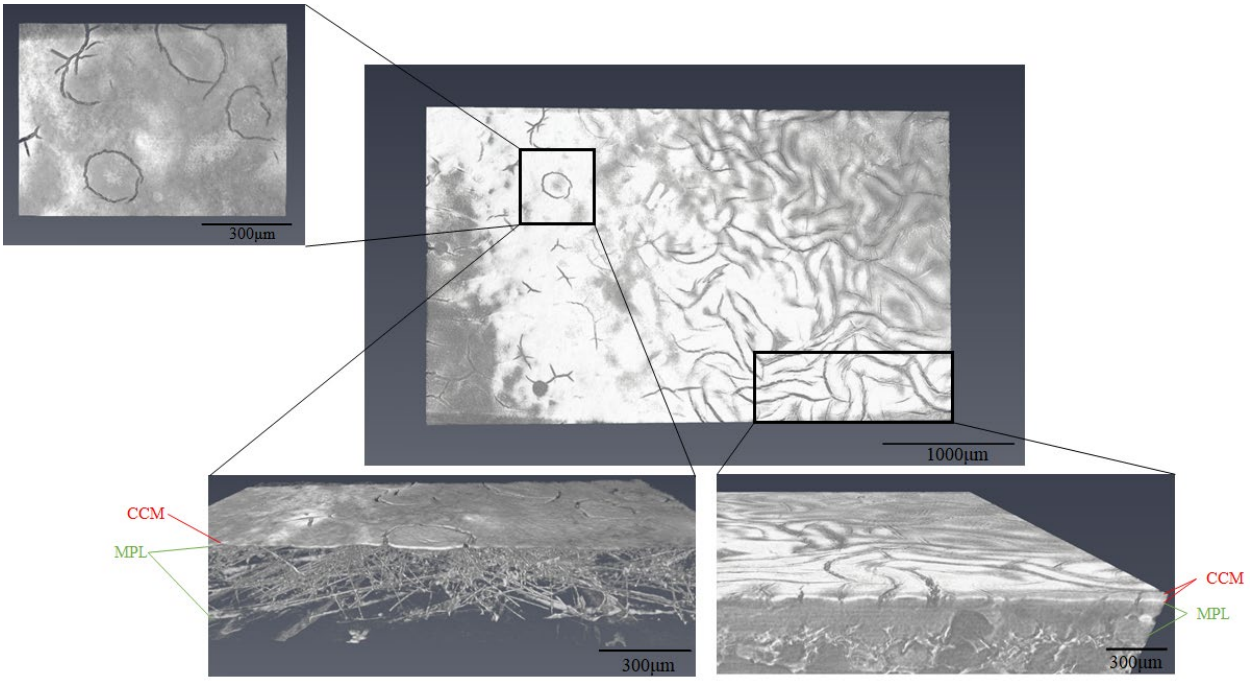

Fig. 7. (a) SEM and (c) XCT images at BOL showing an intact CCM without any crack and delamination. (b) SEM and (d) XCT images showing the cracks on the catalyst layer, partially and fully through the thickness of CCM after the RH cycling test.

3.2 H_2 Crossover versus Test Time

It is also of interest to examine the H_2 crossover with total RH cycling test time for each cycle, which is obtained by multiplying cycle number and cycle duration. These plots are in Fig. 8(a) and Fig. 8(b) for the FCT and CAT cells, respectively. Again, a consistent trend for three groups can be observed for both cell formats. Specifically, the longest cycle (X2 Cycle) leads to the longest overall test time to fail the membrane and the shortest cycle (X0.67 Cycle) leads to the shortest test time, which is contrary to the relative ranking in terms of cycle numbers as discussed for Fig. 4.

Since the H_2 crossover versus time plots exhibit clear separation for the three cycles (Fig. 8), the frequency and duration of cycles both seem to play a role in determining the membrane lifetime, given

the identical time under in-plane tensile stress or dry phase from the three cycles. This finding is in contrast to the existing knowledge that the membrane lifetime is more strongly influenced by the magnitude of tensile stress and accumulation time under stress rather than cycling [8, 17]. Probably the convolution with chemical stress [8] and the ex-situ nature [17] had contributed to these different observations.

To the best of the authors' knowledge, presented here is the first time a state-of-art membrane has failed from RH cycling AST repeatedly with three protocols and two cells, thus providing a unique opportunity to examine its mechanical behaviors thoroughly. It is true that this particular membrane, although a large-volume product and used in a major fuel cell consortium project, seems to lack mechanical stability, as supported by the data in this paper and the supplier's information that it did not pass the DOE RH cycling protocol (2 min / 2 min for 20,000 cycles). However, a long mechanical lifetime of a reinforced membrane should not be always assumed with different design rationales from the suppliers. It is quite likely that the experimental finding from this particular membrane represents a common trend given the similarity of ionomer and reinforcement technologies. That is, both the frequency and duration of cycles have a major impact on the lifetime. Such common trend was not discovered in the literature probably due to the lack of studying the control factors in RH cycling, and the fact that membranes used in previous studies were mechanically too strong to be failed within a reasonable time.

It is believed that the membrane mechanical failure is a damage accrual process, in that the typical in-plane stress in a fuel cell operation is much smaller than the membrane tensile strength. The accrual process from many RH cycles has been modeled as an accumulation of plastic deformation [29] or plastically dissipated energy [30, 31] until reaching a critical amount as the failure. Therefore, the amount or frequency of cycles pertains to the events of adding to the accrual process towards the

failure criterion, as long as the membrane enters the plastic response regime beyond the elastic regime, which is a typical scenario [32]. On the other hand, due to the viscoelastic nature of a membrane, the duration of cycles determines the membrane residual stress during its relaxation, which becomes the initial condition at the transition to the next dry phase and influences the damage accrual process [32-34]. With this analysis, it is not surprising that the frequency and duration of cycles have shown a major impact on the lifetime for three RH cycles in this study. A detailed modeling study on these RH cycles is ongoing towards a future publication and is beyond the scope of this work.

(a)

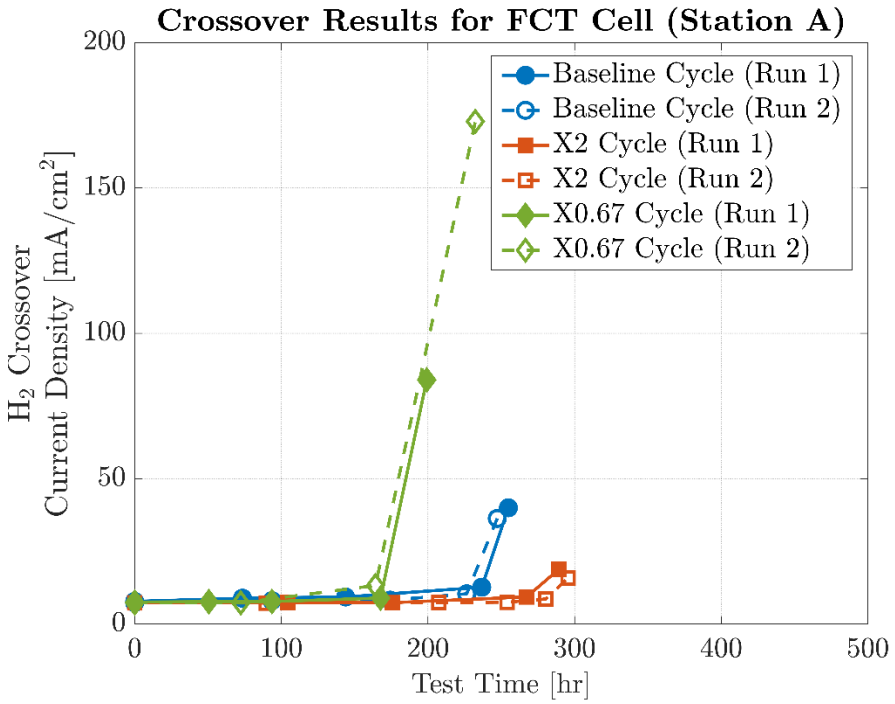

(b)

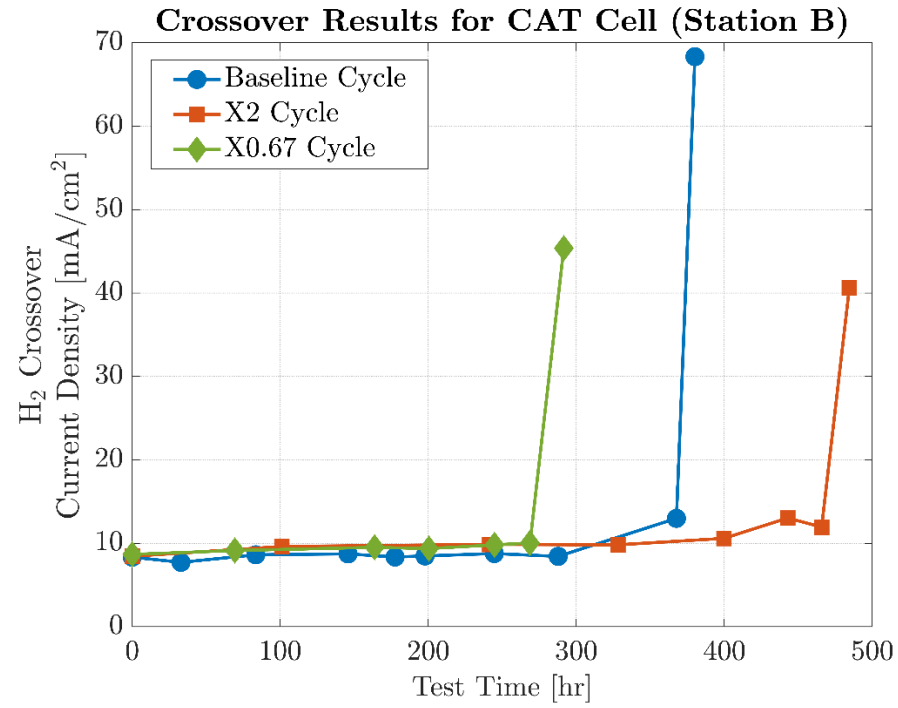

Fig. 8. Evolution of H_2 crossover with RH cycling test hour for three RH cycles on (a) Station A / FCT cell; (b) Station B / CAT cell.

4. Summary and Conclusions

In this study, an experimental design of three RH cycles and two test cell / MEA formats was implemented to evaluate the mechanical durability of a supplier's CCM with a reinforced membrane. To focus on the effect of cycle duration which is an important control factor pertaining to the development of system strategies, the baseline cycle was 45 s dry and 30 s wet, the longer (X2) cycle was 90 s dry and 60 s wet and the shorter cycle (X0.67) was 30 s dry and 20 s wet, in contrast to the traditional DOE RH cycle of 2 min dry and 2 min wet. Model simulations indicate that all three cycles would be able to achieve the desired deep and fast hydration swing, therefore being an effective AST. All 6 RH cycling runs have failed the membrane within three weeks as evidenced by high H_2 crossover, providing a unique, and probably the first-time-in-literature, opportunity to examine the mechanical behaviors of a state-of-art reinforced membrane thoroughly and to propagate the learning towards the development of system strategies for prolonged lifetime.

To confirm the failure, the failed samples were inspected either visually or using XCT and SEM imaging around the failure spots identified from the bubble jig. It was found that RH cycling lifetime on CAT cell was longer than that on FCT cell under the same conditions, in part because the former had all failure spots identified within the active area, whereas the latter failed at the edge of GDL and gasket. It is thus suggested to include the test hardware information, such as MEA gasket and flow field design, along with the RH cycling lifetime, or propagate a hardware harmonization in the community besides the protocol, if the actual lifetimes are used for screening against a target or for comparison. Nevertheless, clear and consistent grouping of three cycles was observed for both test cell / MEA formats with repetitions for FCT cell, indicating that the cyclic fatigue due to hydration cycling is the major contributor to the edge failure. Sharing the same failure mechanism, an RH cycle that is more stressful to the edge, should be also more stressful to the membrane in the active area. Therefore, the difference in test hardware is not expected to impact the outcome if RH cycling is used as a design tool to evaluate a

control factor. In other words, using RH cycling as a design tool emphasizes the sensitivity to the key control factors based on a single set of hardware and material. This sensitivity could be well captured due to the same mechanism regardless of hardware difference. In contrast, using RH cycling as a screening tool focuses on the lifetime result to compare against the target or lifetime from another test, thereby requiring the harmonization of hardware.

With both test cell / MEA formats, X2 Cycle has led to the longest lifetime in RH cycling, although it was associated with the fewest number of cycles to failure. The fact that H_2 crossover versus RH cycling test time plots exhibit clear separation for three cycles, indicates that the frequency and duration of cycles both play a role in determining the membrane lifetime, besides the magnitude of stress and the accumulation time under stress, which contrasts with the existing knowledge in the literature. The findings and insights from this study will enhance the understanding of the RH cycling AST and membrane mechanical durability towards more effective and efficient lifetime screening as well as control strategy development on a fuel cell vehicle.

Acknowledgement:

This research did not receive any specific grant from funding agencies in the public, commercial, or not-for-profit sectors. It is entirely supported by Ford Motor Company. Technical support from Michael Potocki at Ford Motor Company is appreciated.

Reference:

1. H. Tang, P. Shen, S. Jiang, F. Wang, M. Pan, “A degradation study of Nafion proton exchange membrane of PEM fuel cells”, Journal of Power Sources 170, 85-92 (2007).
2. Y.-H. Lai, C. K. Mittelsteadt, C. S. Gittleman, and D. A. Dillard, “Viscoelastic stress analysis of constrained proton exchange membranes under humidity cycling,” Journal of Fuel Cell Science and Technology 6(2), 021002 (2009).
3. A. Kusoglu, M. H. Santare, and A. M. Karlsson, “Aspects of fatigue failure mechanisms in polymer fuel cell membranes,” Journal of Polymer Science Part B: Polymer Physics, 49(21), 1506 (2011).

4. M. Hasan, A. Goshtasbi, J. Chen, M. Santare, T. Ersal, “Model-Based Analysis of PFSA Membrane Mechanical Response to Relative Humidity and Load Cycling in PEM Fuel Cells”, Journal of The Electrochemical Society, 165(6), F3359 (2018).
5. D. Qiu, L. Peng, X. Lai, M. Ni, W. Lehnert, “Mechanical failure and mitigation strategies for the membrane in a proton exchange membrane fuel cell”, Renewable and Sustainable Energy Reviews 113, 109289 (2019).
6. M. Rodgers, L. Bonville , R. Mukundan, R. Borup, R. Ahluwalia, P. Beattie, R. Brooker, N. Mohajeri, H. Kunz, D. Slattery, J. Fenton, “Perfluorinated Sulfonic Acid Membrane and Membrane Electrode Assembly Degradation Correlating Accelerated Stress Testing and Lifetime Testing”, Electrochemical Society Transactions, 58(1), 129 (2013).
7. DOE, Multi-Year Research, Development, and Demonstration Plan, Fuel Cells Section, Page 49 https://www.energy.gov/sites/prod/files/2017/05/f34/fcto_myrdd_fuel_cells.pdf
8. R. Mukundan, A. Baker, A. Kusoglu, P. Beattie, S. Knights, A. Weber, R. Borup, “Membrane Accelerated Stress Test Development for Polymer Electrolyte Fuel Cell Durability Validated Using Field and Drive Cycle Testing”, Journal of The Electrochemical Society, 165(6), F3085-F3093 (2018).
9. K. Panha, M. Fowler, X. Yuan, H. Wang, “Accelerated durability testing via reactants relative humidity cycling on PEM fuel cells”, Applied Energy 93, 90-97 (2012).
10. N. Macauley, A. Alavijeh, M. Watson, J. Kolodziej, M. Lauritzen, S. Knights, G. Wang, E. Kjeang, “Accelerated Membrane Durability Testing of Heavy Duty Fuel Cells”, Journal of The Electrochemical Society 162(1), F98-F107 (2015).
11. S. Vengatesan, M. Fowler, X. Yuan, H. Wang, “Diagnosis of MEA degradation under accelerated relative humidity cycling”, Journal of Power Sources 196, 5045-5052 (2011).
12. B. Huang, Y. Chatillon, C. Bonnet, F. Lapicque, S. Leclerc, M. Hinaje, S. Raël, “Experimental Investigation of Air Relative Humidity (RH) Cycling Tests on MEA/Cell Aging in PEMFC Part I: Study of High RH Cycling Test With air RH at 62%/100%”, Fuel Cells, 12(3), 335 (2012).
13. B. Huang, Y. Chatillon, C. Bonnet, F. Lapicque, S. Leclerc, M. Hinaje, S. Raël, “Experimental Investigation of Air Relative Humidity (RH) Cycling Tests on MEA/Cell Aging in PEMFC Part II: Study of Low RH Cycling Test With air RH at 62%/0%”, Fuel Cells, 12(3), 347 (2012).
14. Y.-H. Lai, K. Rahmoeller, J. Hurst, R. Kukreja, M. Atwan, A. Maslyn, C. Gittleman, “Accelerated Stress Testing of Fuel Cell Membranes Subjected to Combined Mechanical/Chemical Stressors and Cerium Migration”, Journal of The Electrochemical Society 165(6), F3217-F3229 (2018).
15. A. Kusoglu and A. Weber, “Electrochemical/Mechanical Coupling in Ion-Conducting Soft Matter”, The Journal of Physical Chemistry Letters 6, 4547-4552 (2015).
16. A. Alavijeh, R. Khorasany, Z. Nunn, A. Habisch, M. Lauritzen, E. Rogers, G. Wang, E. Kjeang, “Microstructural and Mechanical Characterization of Catalyst Coated Membranes Subjected to In Situ Hygrothermal Fatigue”, Journal of The Electrochemical Society 162(14), F1461-F1469 (2015).
17. Y. Li, D. Dillard, S. Case, M. Ellis, Y.-H. Lai, C. Gittleman, D. Miller, “Fatigue and creep to leak tests of proton exchange membranes using pressure-loaded blisters”, Journal of Power Sources 194, 873-879 (2009).
18. Fuel Cell Technologies, Inc. 50 cm^2 Cell Hardware: http://fuelcelltechnologies.com/single-cell-hardware/cell-hardware/50-square-centimeter-cell-hardware
19. Y. Singh, R. Khorasany, W. Kim, A. Alavijeh, E. Kjeang, R. Rajapakse, G. Wang, “Ex-situ characterization and modeling of fatigue crack propagation in catalyst coated membrane composites for fuel cell applications”, International Journal of Hydrogen Energy 44, 12057-12072 (2019).
20. A. Goshtasbi, P. Garcia-Salaberri, J. Chen, K. Talukdar, D. Sanchez, T. Ersal, “Through-the-membrane transient phenomena in PEM fuel cells – a modeling study”, Journal of The Electrochemical Society, 166, F3154-F3179 (2019).

21. Y. Singh, R, White, M. Najm, T. Haddow, V. Pan, F. Orfino, M. Dutta, E. Kjeang, “Tracking the evolution of mechanical degradation in fuel cell membranes using 4D in situ visualization”, Journal of Power Sources 412, 224-237 (2019).
22. D. Ramani, Y. Singh, R, White, M. Wegener, F. Orfino, M. Dutta, E. Kjeang, “4D in-situ visualization of mechanical degradation evolution in reinforced fuel cell membranes”, International Journal of Hydrogen Energy 45, 10089-10103 (2020).
23. J. Hack, T. Heenan, F. Iacoviello, N. Mansor, Q. Meyer, P. Shearing, N. Brandon, D. Brett, “A structure and durability comparison of membrane electrode assembly fabrication methods: self-assembled versus hot-pressed”, Journal of The Electrochemical Society, 165, F3045-F3052 (2018).
24. N. Kulkarni, M. Kok, R. Jervis, F. Iacoviello, Q. Meyera, P. Shearing, D. Brett, “The effect of non-uniform compression and flow-field arrangements on membrane electrode assemblies—X-ray computed tomography characterization and effective parameter determination”, Journal of Power Sources 426, 97-110 (2019).
25. X. Huang, R. Solasi, Y. Zou, M. Feshler, K. Reifsnider, D. Condit, S. Burlatsky, T. Madden, “Mechancial endurance of polymer electrolyte membrane and PEM fuel cell durability”, Journal of Polymer Science Part B: Polymer Physics 44, 2346–2357 (2006).
26. R. Solasi, Y. Zou, X. Huang, K. Reifsnider, D. Condit, “On mechanical behavior and in-plane modeling of constrained PEM fuel cell membranes subjected to hydration and temperature cycles”, Journal of Power Sources 167, 366-377 (2007).
27. D. Bograchev, M. Gueguen, J.-C. Grandidier, S. Martemianov, “Stress and plastic deformation of MEA in running fuel cell”, International Journal of Hydrogen Energy 33, 5703-5717 (2008).
28. T. Ralph, D. Barnwell, P. Bouwman, A. Hodgkinson, M. Petch, M. Pollington, “Reinforced Membrane Durability in Proton Exchange Membrane Fuel Cell Stacks for Automotive Applications”, Journal of The Electrochemical Society 155, B411-B422 (2008).
29. S.F. Burlatsky, M. Gummalla, J. O’Neill, V.V. Atrazhev, A.N. Varyukhin, D.V. Dmitriev, N.S. Erikhman, “A mathematical model for predicting the life of polymer electrolyte fuel cell membranes subjected to hydration cycling”, Journal of Power Sources 215, 135-144 (2012).
30. G. Ding, M. Santare, A. Karlsson, A. Kusoglu, “Numerical evaluation of crack growth in polymer electrolyte fuel cell membranes based on plastically dissipated energy”, Journal of Power Sources 316, 114-123 (2016).
31. M. Hasan, J. Chen, J. Waldecker, Y. Singh, E. Kjeang, M. Santare, “Determining the critical plastically dissipated energy for fatigue crack growth in PEM fuel cell membrane and its environmental sensitivity”, International Journal of Fatigue 138, 105697 (2020).
32. A. Kusoglu, M. Santare, A. Karlsson, S. Cleghorn, W. Johnson, “Numerical Investigation of Mechanical Durability in Polymer Electrolyte Membrane Fuel Cells”, Journal of The Electrochemical Society 157, B705-B713 (2010).
33. N. Khattra, A. Karlsson, M. Santare, P. Walsh, F. Busby, “Effect of time-dependent material properties on the mechanical behavior of PFSA membranes subjected to humidity cycling”, Journal of Power Sources 214, 365-376 (2012).
34. N. Khattra, Z. Lu, A. Karlsson, M. Santare, F. Busby, T. Schmiedel, “Time-dependent mechanical response of a composite PFSA membrane”, Journal of Power Sources 228, 256-269 (2013).